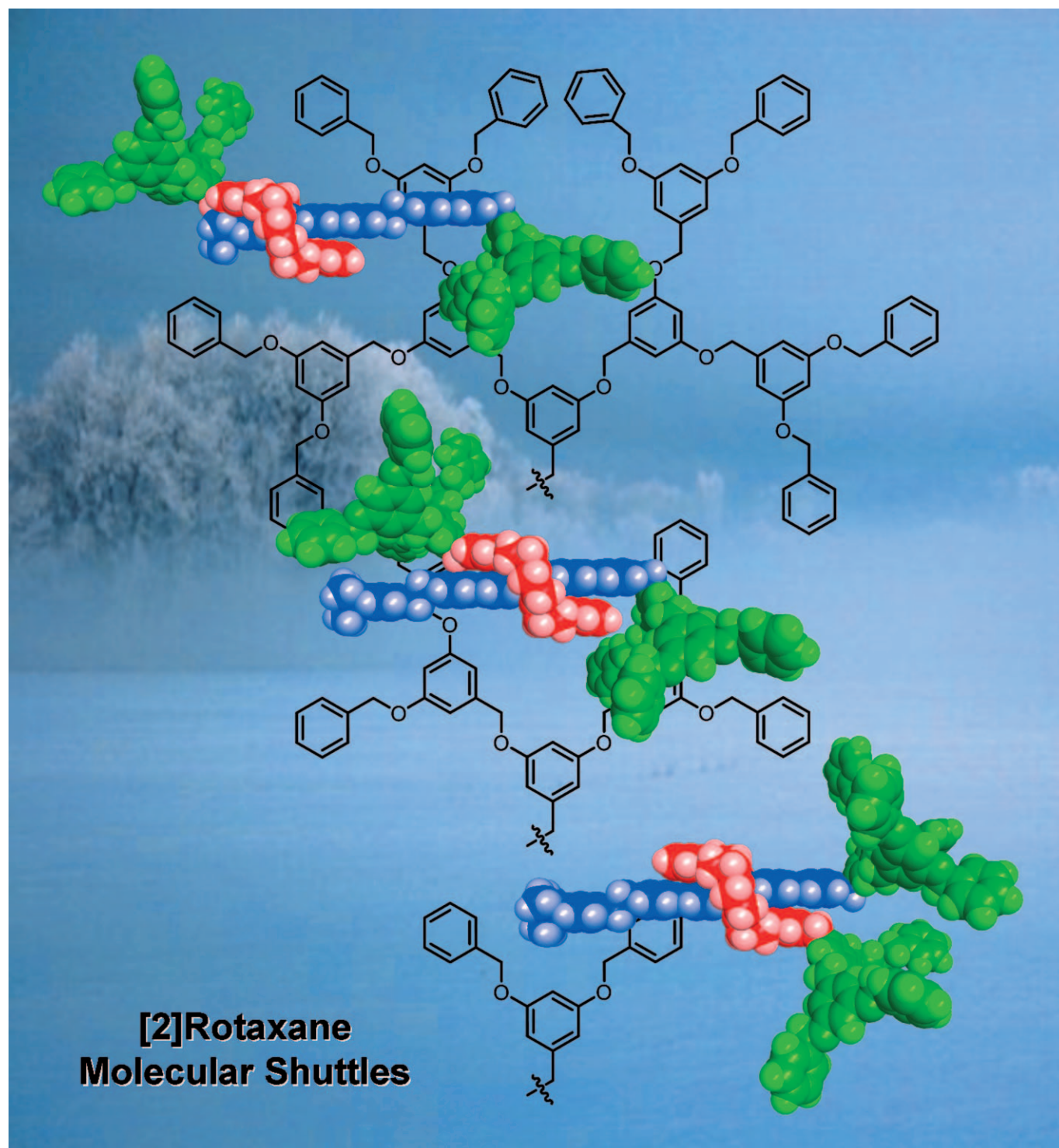


The Effect of Incorporating Fréchet Dendrons into Rotaxanes and Molecular Shuttles Containing the 1,2-Bis(pyridinium)ethane \subset [24]Crown-8 Templating Motif

David A. Tramontozzi, Natalie D. Suhan, S. Holger Eichhorn, and Stephen J. Loeb*^[a]



Abstract: Fréchet-type dendrons (G0–G3) were added as both axle stoppering units and cyclic wheel appendages in a series of [2]rotaxanes, [3]rotaxanes, and molecular shuttles that employ 1,2-bis(pyridinium)ethane axles and 24-membered crown ethers wheels. The addition of dendrimer wedges as stoppering units dramatically increased the solubility of simple [2]rotaxanes in nonpolar solvents. The X-ray structure

of a G1-stoppered [2]rotaxane shows how the dendritic units affect the structure of the interlocked components. Increased solubility allows observation of how the interaction of dendritic units on separate components in interlocked

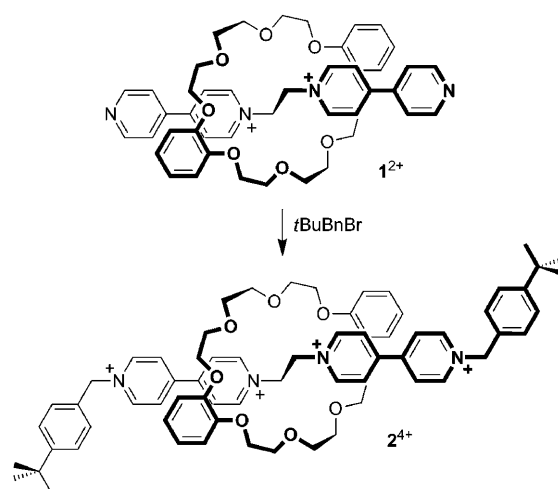
molecules influences switching properties and molecular size. In a series of [2]rotaxane molecular shuttles incorporating two recognition sites, it was demonstrated that an increase in generation on either the stoppering unit or cyclic wheel could influence both the rate of shuttling and the site preference of the wheel on the axle.

Keywords: dendrimers • molecular machines • molecular shuttles • rotaxanes

Introduction

A fundamental understanding of the dynamic nature of mechanically interlocked molecules has led to the design and construction of a number of chemical systems that display basic machine-like properties at the molecular level.^[1] To transform interlocked molecules such as [2]rotaxanes or [2]catenanes into molecular machines, these systems must be capable of accessing two or more distinct molecular arrangements (coconformations) and undergoing a simple process that allows switching between the two states.^[2] Although there are a number of well-defined and understood examples that operate in solution,^[1] the incorporation of molecular machinery into modern materials requires combining the properties of these two relatively disparate chemical worlds and understanding this interface.^[3] Strategies that lead to the fabrication of solid-state nanoscale devices from interlocked molecules have been investigated,^[1a] but there still remains a great deal to learn before we can produce functional materials driven by molecular machinery.^[4]

As a first step towards incorporating interlocked molecules based on the 1,2-bis(pyridinium)ethane/[24]crown-8 template^[5] (Scheme 1) into materials, we have focused on elaborating this small-molecule chemistry for the generation of liquid crystalline and polymeric materials. Herein, we report the results of incorporating Fréchet-type dendrons^[6] into [2]rotaxanes and [2]rotaxane molecular shuttles. In particular, the attachment of dendritic units to both the linear and cyclic components of a molecular shuttle results in a large difference in size between the two coconformations. The effect of these changes on molecular shuttling and coconformational distribution is described.^[7]

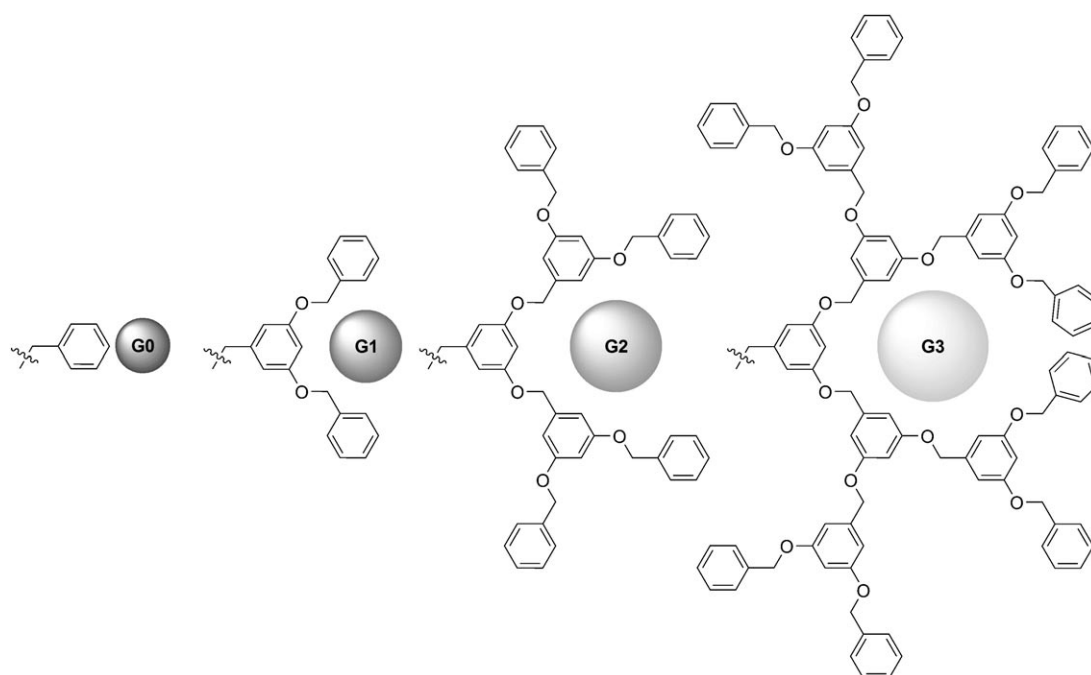


Scheme 1. A linear 1,2-bis(4,4'-bipyridinium)ethane dication and a dibenzo[24]crown-8 (**DB24C8**) macrocycle act as axle and wheel to form the interpenetrated [2]pseudorotaxane, **1**²⁺ (top). This can be converted into a fully interlocked [2]rotaxane, **2**²⁺, by alkylation with bulky capping groups, such as *t*Bu-benzyl (bottom). Anions are not shown but are PF₆ throughout unless otherwise noted.

Results and Discussion

[2]Rotaxanes containing a DB24C8 wheel and Fréchet-type dendrimer stoppers: The first step in incorporating Fréchet-type polyaryl ether units into 1,2-bis(pyridinium)ethane/[24]crown-8 interlocked molecules involved using various generations (Scheme 2) to stopper [2]rotaxanes containing a simple **DB24C8** wheel.^[8] This provided a baseline for gauging the changes in basic physical properties, primarily solubility. A series of [2]rotaxanes were prepared that were identical to compound **2** (Scheme 1), except that different generations (G1, G2, G3) of dendrimeric wedges were used in place of *tert*-butylbenzyl and that groups (G0 and G1) were also appended to the crown ether. ¹H NMR spectroscopy and ESIMS verified the purity and identity of each [2]rotaxane. These are designated by the generations used in their construction in the order first axle stopper, wheel appendage, second axle stopper; for example, [2]rotaxane [**G3-**

[a] Dr. D. A. Tramontozzi, Dr. N. D. Suhan, Prof. S. H. Eichhorn, Prof. S. J. Loeb
Department of Chemistry and Biochemistry
University of Windsor, Windsor, ON, N9B 3P4 (Canada)
Fax: (+1) 519-973-7098
E-mail: loeb@uwindsor.ca



Scheme 2. The various Fréchet-type dendritic wedges (G0, G1, G2, G3) used in this study as stoppers for the pyridinium axles and appendages on the crown ether wheels. When there is no appendage on the crown ether, that is, for **DB24C8**, the code used is “H”.

G1-G3⁴⁺ has G3 stoppering units on each end of the axle with a G1 appendage on the crown ether wheel.

The single-crystal X-ray structure of the [2]rotaxane [**G1-H-G1**]⁴⁺ is shown in Figure 1. The two stoppering units are oriented on opposite sides of the central linear portion, which adopts the same basic conformation previously observed when *tert*-butylbenzyl stoppering units were used.^[9] The presence of these larger stoppering units has no significant structural effect on the interactions between the pyridinium axle and the crown ether wheel.^[10] Even the addition of larger generations (G2 and G3) showed no changes to the ¹H NMR spectra (other than increased intensity for the aryl ether resonances) and it was concluded that the stoppering wedges extend away from the core and therefore exert little effect on the interlocked core of the structure.

The addition of dendrimer stoppering groups did however have significant effect on the solubility of the [2]rotaxanes and the material properties of the solid. The original rotaxane **2** and [**G1-H-G1**]⁴⁺ are soluble in most polar organic solvents, such as DMSO, DMF, MeOH, CH₃NO₂, and MeCN, but not in less polar ones. Addition of larger dendrimers allowed dissolution of the rotaxane structure in less polar solvents to the extent that [**G1-G1-G1**][PF₆]₄ is soluble in acetone, [**G2-G1-G2**][PF₆]₄ in CH₂Cl₂ and CHCl₃, and [**G3-G1-G3**][PF₆]₄ in THF and even benzene and toluene (see Figure 2).

The fact that a tetracationic species can be manipulated to the point that it becomes soluble in toluene shows the extent to which addition of dendrimer stoppers can change the physical properties of these molecules without apparently altering significantly the structure of the interlocked core.

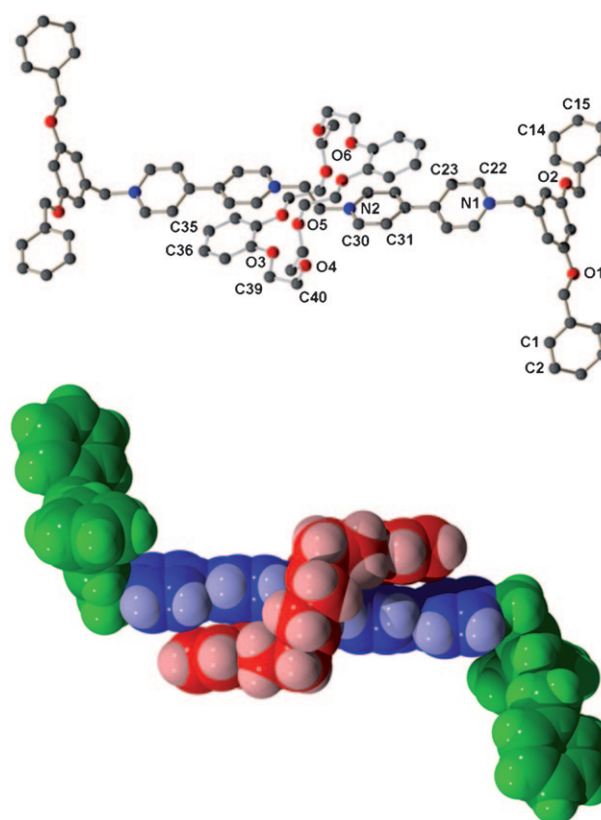


Figure 1. X-ray structure of the [2]rotaxane [**G1-H-G1**]⁴⁺. Top: A ball-and-stick representation with the numbering scheme depicted. Bottom: A space-filling view: pyridinium axle = blue, crown ether wheel = red, G1 dendrimeric stoppering unit = green. There is a crystallographically imposed center of symmetry.

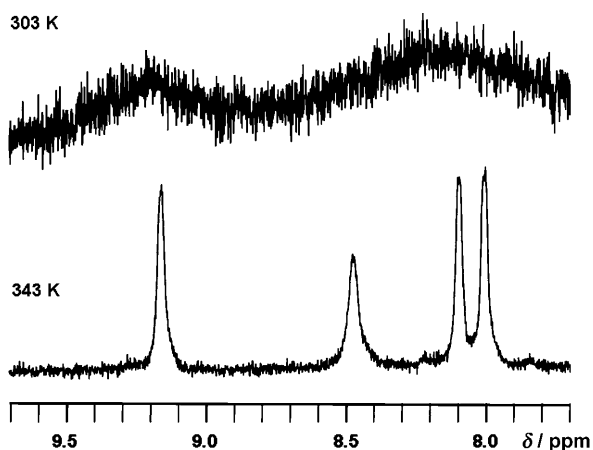


Figure 2. ^1H NMR spectra of $[\text{G3-G1-G3}]^{4+}$ in $[\text{D}_8]$ toluene at 303 (top) and 343 K (bottom) showing the four pyridinium resonances on the axle.

A clue to how this occurs comes from changes in the ^1H NMR spectra in a single solvent, MeCN, as the complexity of the rotaxane is varied from $[\text{G1-H-G1}]^{4+}$ to $[\text{G3-G1-G3}]^{4+}$. The pyridinium proton closest to the dendrimer stopper is exposed to surrounding solvent to the greatest extent. As the generation size is increased, this hydrogen atom is shielded more from the polar solvent by the organic groups of the dendrimer and systematically shifts upfield as a result; $\delta = 8.92$ ppm for $[\text{G1-H-G1}]^{4+}$ to $\delta = 8.78$ ppm for $[\text{G3-G1-G3}]^{4+}$. One can imagine with G3 stoppers and a G1 appendage on the crown that the dendrimer wedges of $[\text{G3-G1-G3}]^{4+}$ completely encapsulate the charged core. This probably limits the direct interaction of the pyridinium nitrogen atoms with solvent molecules and, along with reduced charge density and weakened cohesion in the solid state, leads to an increase in solubility in nonpolar media, such as toluene or benzene.

Interestingly, the ^1H NMR spectrum of $[\text{G3-G1-G3}]^{4+}$ in $[\text{D}_8]$ toluene at room temperature (303 K) is extremely broad, whereas raising the temperature to 343 K yields a spectrum essentially identical to that seen in more polar solvents (Figure 2). As described above, it is likely that upon dissolution in this very nonpolar solvent the peripheral dendrimer units fold back around the polar core resulting in a more globular-shaped molecule, which causes the relative motion of the rotaxane components to be hindered. When interconversion between the available conformations is close to the NMR timescale, very broad signals are observed as shown in Figure 2 (top) for $[\text{G3-G1-G3}]^{4+}$ at 303 K in $[\text{D}_8]$ toluene. At high temperature (343 K), the rate of interconversion between the available conformations is fast on the NMR timescale and only sharp averaged signals are observed.

Figure 3 shows a molecular mechanics^[11] derived model of the $[\text{G3-H-G3}]^{4+}$ rotaxane in space-filling mode. Even in this relatively idealized conformation, it is fairly clear that the very large G3 stoppering units almost completely encapsulate the core.

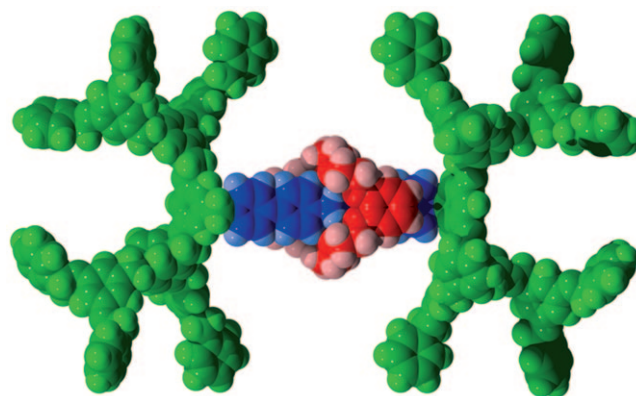


Figure 3. A molecular mechanics derived space-filling model of the $[\text{G3-H-G3}]^{4+}$ rotaxane.

Materials properties of rotaxanes with dendritic stoppers:

The addition of Fréchet dendrons had a significant effect on the solution behavior of these rotaxanes and since the introduction of these bulky groups has the potential to impart mesomorphic properties to the solid state, we also decided to undertake a preliminary investigation of their basic materials properties. The mesomorphism of $[\text{G1-H-G1}][\text{PF}_6]_4$, $[\text{G2-H-G2}][\text{PF}_6]_4$, and $[\text{G3-H-G3}][\text{PF}_6]_4$ were studied by polarized optical microscopy (POM), thermogravimetric analysis (TGA), differential scanning calorimetry (DSC), and X-ray diffraction (XRD).

$[\text{G1-H-G1}][\text{PF}_6]_4$, $[\text{G2-H-G2}][\text{PF}_6]_4$, and $[\text{G3-H-G3}][\text{PF}_6]_4$ are thermally stable to $\approx 190^\circ\text{C}$ under inert gas based on the onset temperature of weight loss determined by thermal gravimetric analysis at a heating rate of 2°C min^{-1} . Since it is the bond between the pyridinium unit of the thread and the benzylic methylene group of the stopper that is thermally most labile, it is not surprising that $[\text{G1-H-G1}][\text{PF}_6]_4$, $[\text{G2-H-G2}][\text{PF}_6]_4$, and $[\text{G3-H-G3}][\text{PF}_6]_4$ all decompose at about the same temperature, as confirmed by POM. It should be noted that this decomposition temperature is $\approx 30^\circ\text{C}$ higher than the values reported for derivatives of *N,N*-dibenzyl-substituted 4,4'-bipyridine (viologen). This stabilizing effect could be attributed to protection of the viologen unit by the attached crown ether, but since there is no difference in stability between $[\text{G1-H-G1}][\text{PF}_6]_4$, $[\text{G2-H-G2}][\text{PF}_6]_4$, and $[\text{G3-H-G3}][\text{PF}_6]_4$ this effect cannot be related to the incorporation of the different dendrons.

All three rotaxanes showed second-order phase transitions between 80 – 100°C in the DSC graphs that coincide with softening temperatures of mechanically sheared samples observed by POM. Transitions from the birefringent to the isotropic state occur over wide temperature ranges of 173 – 181°C for $[\text{G1-H-G1}][\text{PF}_6]_4$, 139 – 149°C for $[\text{G2-H-G2}][\text{PF}_6]_4$, and 116 – 129°C for $[\text{G3-H-G3}][\text{PF}_6]_4$ and were not resolved in the DSC graphs. It must be stated here that the samples are highly viscous even in their isotropic phase, which explains why the transition into the isotropic states (clearing) occur over wide temperature ranges. The high vis-

cosity is also the reason why the birefringence requires several days to develop upon cooling from the isotropic state.

Two broad reflections dominate the XRD patterns of all three compounds and are indicative of nematic mesophases and the observed schlieren-type defect textures agree with this assignment (see Figure 4), however, texture analysis is

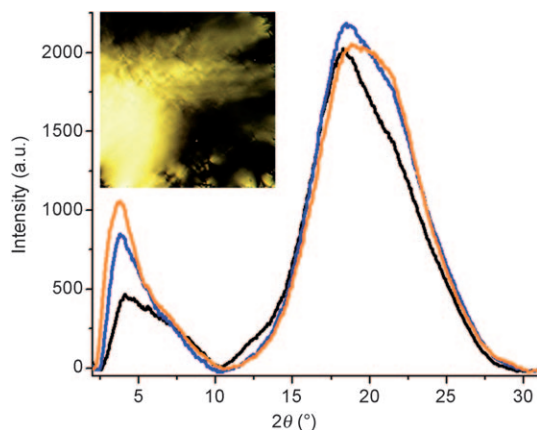
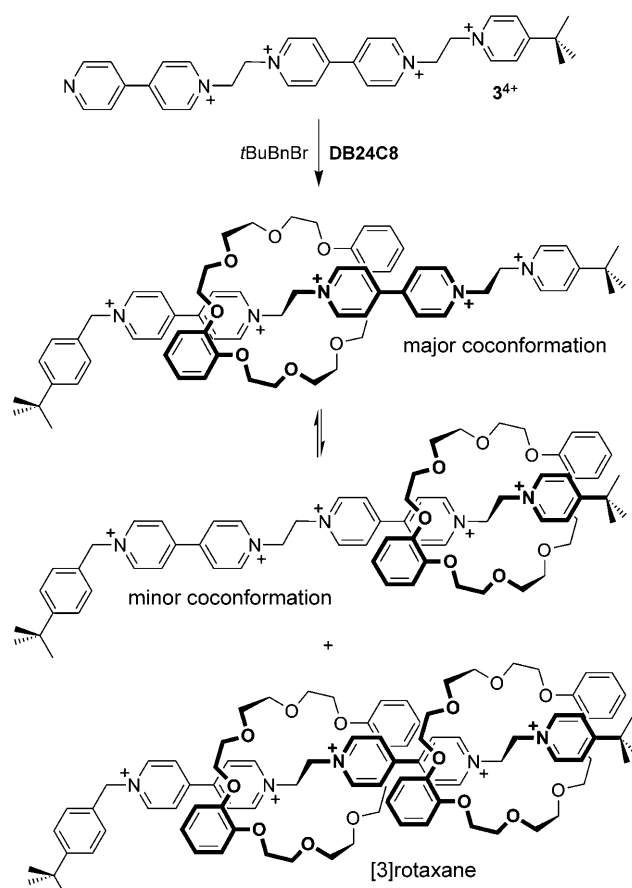


Figure 4. XRD patterns of [G1-H-G1][PF₆]₄ (black), [G2-H-G2][PF₆]₄ (blue), and [G3-H-G3][PF₆]₄ (orange) in their nematic glass phases at 22 °C. Inserted is a POM image of the texture of [G2-H-G2][PF₆]₄ at 105 °C.

complicated by the high viscosity of these compounds. The maxima of the small-angle reflections between 21 and 24 Å agree with the approximate lengths of the rotaxanes and the wide-angle reflections between 4 and 5 Å represent the typical packing distances of aliphatic and aromatic groups. All small-angle peaks show shoulders between 11 and 16 Å that agree with the estimated lateral packing distance of the molecules. Amorphous Fréchet dendrons have been shown to give a broad reflection at 5 Å, whereas the packing distances of aromatic units in the core is expected at around 4 Å.

Molecular shuttles containing Fréchet-type dendrimer units on both the DB24C8 wheel and stoppering unit: The most widely studied type of molecular switch based on interlocked molecules is the [2]rotaxane molecular shuttle pioneered by Stoddart et al.^[12] In a molecular shuttle, two different recognition sites are present on the axle for the binding of a single macrocyclic wheel. The two coconformations are translational isomers related by the relative positioning of the two interlocked components.

In an earlier study, we showed that by extending our 1,2-bis(pyridinium)ethane[24]crown-8 template so that the axle contained two recognition sites, both [3]- and [2]rotaxane molecular shuttles could be prepared. Scheme 3 shows a [2]rotaxane molecular shuttle with two different bis(pyridinium)ethane binding sites and a single molecule of DB24C8.^[14] Since only one set of ¹H NMR resonances was observed for the axles at room temperature, it was concluded that the DB24C8 molecule was undergoing fast exchange between the two binding sites. From variable-temperature



Scheme 3. A [2]rotaxane molecular shuttle can be created in which the cyclic wheel (shown here as DB24C8) can shuttle rapidly between two different 1,2-bis(pyridinium)ethane recognition sites on the same axle. During the synthesis of these [2]rotaxanes, a corresponding [3]rotaxane is also produced that contains two of the crown ethers utilized in the preparation (shown here as DB24C8).

(VT)-NMR spectral data, it was determined that the barrier to shuttling was 54 kJ mol⁻¹ and the ratio of site occupancy was determined to be 65:35 in favor of the 1,2-bis(4,4'-bipyridinium)ethane site over the site terminated in a 4-*tert*-butylpyridinium group;^[13] see Scheme 3 for designations of major and minor translational isomers.

To study the effect of dendrimer incorporation on molecular shuttling, we synthesized a series of [2]rotaxanes that contain G1 or G2 stoppers on one end of the axle and as the cyclic component a DB24C8 derivative, that is, [G1-H]⁵⁺, [G1-G0]⁵⁺, [G1-G1]⁵⁺, [G1-G2]⁵⁺, [G2-H]⁵⁺, [G2-G0]⁵⁺, [G2-G1]⁵⁺, and [G2-G2]⁵⁺. As outlined in Scheme 3, an unintentional but inevitable byproduct in each of these preparations was the corresponding [3]rotaxane,^[14] that is, [G1-H/H]⁵⁺, [G1-G0/G0]⁵⁺, [G1-G1/G1]⁵⁺, [G1-G2/G2]⁵⁺, [G2-H/H]⁵⁺, [G2-G0/G0]⁵⁺, [G2-G1/G1]⁵⁺, and [G2-G2/G2]⁵⁺. The [3]rotaxanes were isolated by column chromatography and characterized by NMR spectroscopy and mass spectrometry (see the Experimental Section), but due to the small amounts produced no further details are reported herein.

Previously reported studies incorporating dendritic units into molecular shuttles focused exclusively on systems in which the dendrimers were part of the stoppering groups.^[7a] As a result, fundamental characteristics of a molecular shuttle, such as coconformational preference and shuttling rate for the macrocycle, were really no different than in analogous systems with conventional stoppers. In contrast, the molecular shuttles presented in this study contain a significant increase in structural complexity. Since the dendritic units are attached to both the axle and wheel components, the two possible coconformations have dramatically different sizes and shapes and for the first time coconformational preference and shuttling rate can be correlated to the size of the molecular units involved. The ability to significantly reorganize the shape of a macromolecular species by switching the components of an interlocked core at the molecular level may find interesting applications in polymer chemistry^[15] and may also provide insight into the fundamental nature of biological macromolecules, which are known to rely heavily on changes in shape for their function.^[16]

The eight new molecular shuttles were isolated and characterized by ¹H NMR spectroscopy and ESIMS (see the Supporting Information). Each was then investigated by VT ¹H NMR spectroscopy and the experimental data simulated^[17] to determine rates of exchange between the two recognition sites. The *t*Bu peaks were used for analysis because these were easily identified singlets in a noncrowded portion of the spectrum. In each case, at room temperature a single peak was observed. This broadened as the temperature was lowered, eventually coalescing and then splitting into two separate resonances at the lowest temperatures. Direct integration of the low-temperature limiting resonances allowed measurement of a site occupancy ratio. The results are summarized in Table 1.

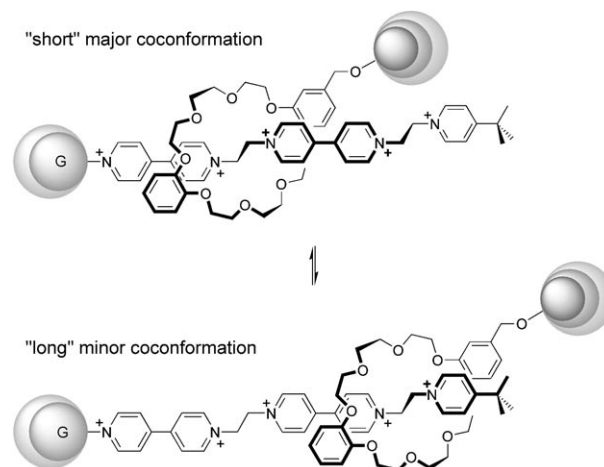
Table 1. Results of VT ¹H NMR spectroscopy studies on dendritic molecule shuttles.^[a]

Stoppering unit	Crown appendage	Barrier to shuttling [kJ mol ⁻¹]	Site occupancy ratio ^[b]
H	H	54	67:33 ^[c]
G1	H	58	78:22
G1	G0	64	83:17
G1	G1	69	85:15
G1	G2	72	88:12
G2	H	68	79:21
G2	G0	70	83:17
G2	G1	71	87:13
G2	G2	84	88:12

[a] NMR spectra were recorded in [D₃]MeCN. Energy barriers and rates were obtained from simulations using the program gNMR.^[17] [b] Occupancy ratios were determined from direct integration of *t*Bu resonances. The ratio refers to major/minor as pictured in Scheme 4. [c] Data from reference [13].

There are two clear trends: 1) as the size of the dendritic wedges increase on either the stopper or the wheel, the barrier to shuttling increases, thus decreasing the rate of shuttling, and 2) there is a concomitant increasing preference for

the more compact “short” version of the molecule, which has the crown ether wheel situated on the 1,2-bis(4,4'-bipyridinium)ethane recognition site (Scheme 4).



Scheme 4. The incorporation of dendrons onto both the axle and the wheel of a [2]rotaxane molecular shuttle dramatically influences the size of the two possible coconformations.

For the barrier to translational motion to increase, there must be an extra energy cost associated with shuttling. As the dendritic wedge size increases, there is likely to be more shielding of the rotaxane core by the large organic fragments. This could create a microenvironment at the recognition site that would be more favorable for the noncovalent interactions between axle and wheel. This would be akin to reducing the polarity of the solvent, which is already known to have a dramatic effect on shuttling rates. However, another factor that must be taken into account is the observation that there is a preference for the “short” coconformation. It may be that there are positive forces stabilizing this coconformation. As estimated by molecular mechanics calculations, there is a difference of >1 nm in length between the long and short versions of the molecule (≈ 42 versus ≈ 54 Å) equal to the distance between the two recognition sites.^[19] From a thermodynamic point of view, the more compact molecule might be favorable, since it simply requires less solvation, but another factor that could contribute to stabilizing the smaller isomer is the formation of an arrangement of axle and wheel, as shown in Figure 5. As the dendritic wedges increase in size, there would be an increased likelihood of interdigitation of the aromatic rings which would add to the noncovalent interactions to be overcome to facilitate shuttling.

Conclusion

We have shown that adding Fréchet-style dendrons to the stoppering groups of [2]rotaxanes will allow their dissolution in very nonpolar solvents such as toluene. This may have utility for depositing these compounds on substrates, for ex-

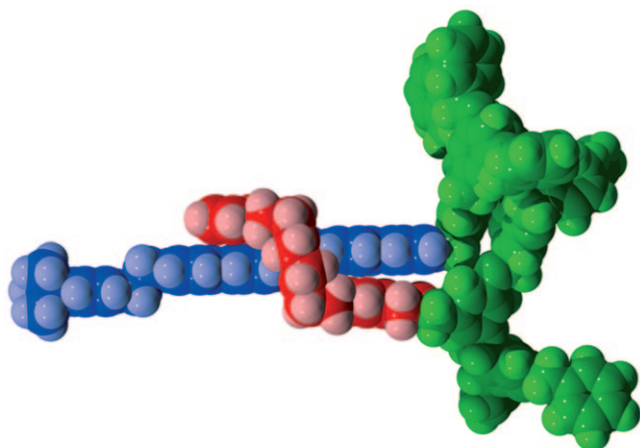


Figure 5. A molecular mechanics (MM3) derived space-filling model showing how interdigitation of the dendrons on the axle and wheel could act as a stabilizing interaction to favor this more compact [2]rotaxane conformation.

ample, in the production of thin films. We also reported that the addition of these large organic groups leads to materials that are soft and show simple alignment in the solid state. Most importantly, we have demonstrated that incorporating large dendritic fragments into the components of a molecular shuttle increases the barrier to shuttling and skews the distribution of coconformations in favor of a single recognition site. Since the shuttling event causes a dramatic change in the shape of the molecule, this also demonstrates the potential of using interlocked components to manipulate the shape of macromolecules. One can envisage using a bistable molecular shuttle as the core machinery to open and close large capsules or perhaps even initiate a macroscopic phase change under the right circumstances.

Experimental Section

General: [18]Crown-6, benzyl bromide, carbon tetrabromide, 3,5-dihydroxybenzyl alcohol, sodium hydride, tetrabutyl ammonium iodide (TBAI), triphenylphosphine, ammonium chloride, ammonium hexafluorophosphate, catechol, cesium carbonate, 2-[2-(2-chloroethoxy)ethoxy]ethanol, 1,2-dibromoethane, 3,4-dihydroxybenzaldehyde, 4,4'-dipyridyl, magnesium sulfate, 4-methylpyridine, 4-phenylpyridine, potassium carbonate, pyridine, sodium borohydride, thionyl chloride, *p*-toluenesulfonyl chloride, and 4-trifluoromethylpyridine were purchased from Aldrich and used as received. All [2]rotaxanes were prepared as the hexafluorophosphate (PF_6^-) salts unless otherwise noted. Deuterated solvents were obtained from Cambridge Isotope Laboratories and used as received. Solvents were dried by using an Innovative Technologies Solvent Purification System. TLC was performed by using Merck Silica gel 60 F_{254} plates and viewed under UV light. Column chromatography was performed by using Silicycle Ultra Pure Silica Gel (230–400 mesh). ^1H NMR experiments were performed on a Bruker Avance 500 instrument operating at 500.1 MHz. The deuterated solvent was used as the lock and the residual solvent or TMS as the internal reference. Conventional 2D NMR experiments (^1H - ^1H COSY and NOESY) were used to assign all peaks. Diagrams and tables showing the assignments for all ^1H NMR resonances are provided in the accompanying Supporting Information. High-resolu-

tion mass spectrometry (HRMS) experiments were performed on a Micromass-LCT electrospray (ES) time-of-flight (TOF) mass spectrometer. Solutions of 50–100 $\mu\text{g mL}^{-1}$ were prepared in 1:1 MeCN/ H_2O (unless otherwise indicated), and injected for analysis at a rate of 5 $\mu\text{L min}^{-1}$ using a syringe pump. Aryl ether dendrons,^[18] 3-hydroxymethylbenzo[24]-crown-8 ether,^[19] and axles 1,2-bis(4,4'-bipyridinium)ethane[PF_6]₂^[20] and 3[PF_6]₄^[21] were synthesized as previously reported in the literature.

Synthesis of G0-DB24C8: 3-Hydroxymethylbenzo[24]crown-8 ether (0.461 g, 0.963 mmol) and benzylbromide (0.267 g, 1.56 mmol) were added to a suspension of sodium hydride (0.253 g, 10.5 mmol) in dry THF (50 mL) and the mixture was heated at reflux for 3 d under a nitrogen atmosphere. Water (30 mL) was slowly added to quench the reaction and the product was extracted into CH_2Cl_2 (3 \times 20 mL). The organic layers were combined, dried (anhydrous MgSO_4), filtered, and concentrated. The residue was subjected to column chromatography; SiO_2 , CH_2Cl_2 and then methanol was added to elute the last compound. Like fractions were combined and then concentrated to yield a yellow oil, which was subsequently dissolved in CHCl_3 (3 mL). Hexanes were added to precipitate **G0-DB24C8** as a white solid (0.471 g, 86%). ^1H NMR (CDCl_3): δ = 7.33–7.14 (m, 5H), 6.89–6.81 (m, 7H), 4.51 (s, 2H), 4.45 (s, 2H), 4.15–4.13 (m, 8H), 3.91–3.89 (m, 8H), 3.82 ppm (s, 8H); HRMS (ESI): m/z calcd for [**G0-DB24C8**+Na]⁺: 591.2570; found: 591.2592.

Synthesis of G1-DB24C8: The same procedure as that used for **G0-DB24C8** was used with bromomethyl-**G1** in place of benzylbromide to yield **G1-DB24C8** as a white solid (0.748 g, 90%). ^1H NMR (CDCl_3): δ = 7.42–7.31 (m, 10H), 6.90–6.83 (m, 7H), 6.62 (d, 4J = 1.3 Hz 2H), 6.56 (t, 4J = 1.3 Hz, 1H), 5.03 (s, 4H), 4.46 (s, 2H), 4.44 (s, 2H), 4.16–4.13 (m, 8H), 3.92–3.89 (m, 8H), 3.83–3.82 ppm (m, 8H); HRMS (ESI): m/z calcd for [**G1-DB24C8**+Na]⁺: 803.3407; found: 803.3372.

Synthesis of G2-DB24C8: The same procedure as that used for **G0-DB24C8** was used with bromomethyl-**G2** in place of benzylbromide to yield **G2-DB24C8** as a yellow oil (1.007 g, 96%). ^1H NMR (CDCl_3): δ = 7.45–7.33 (m, 20H), 6.91–6.83 (m, 7H), 6.70 (d, 4J = 2.2 Hz, 4H), 6.59 (t, 4J = 2.2 Hz, 2H), 6.62 (d, 4J = 2.2 Hz, 2H), 6.53 (t, 4J = 2.2 Hz, 1H), 5.05 (s, 8H), 4.99 (s, 4H), 4.47 (s, 2H), 4.45 (s, 2H), 4.18–4.12 (m, 8H), 3.94–3.89 (m, 8H), 3.84–3.83 ppm (m, 8H); HRMS (ESI): m/z calcd for [**G2-DB24C8**+Na]⁺: 1227.5082; found: 1227.5071.

Synthesis of rotaxane [G1-H-G1][PF₆]₄: 1,2-Bis(4,4'-bipyridinium)ethane[PF_6]₂ (0.070 g, 0.111 mmol), bromomethyl-**G1** (0.176 g, 0.461 mmol), **DB24C8** (0.102 g, 0.227 mmol), and a catalytic amount of TBAI (15 mg) were dissolved in MeNO_2 (10 mL). Water (10 mL) and a saturated aqueous solution of NH_4PF_6 (2 mL) were added and the two-layer reaction was stirred at room temperature for 21 d (at 7 and 14 d the aqueous layer was replaced with fresh distilled water). The organic layer was separated, dried (anhydrous MgSO_4), concentrated (2 mL), and precipitated with diethyl ether. The precipitate was filtered through Celite and washed into a clean flask with MeCN. The solvent was evaporated and the red/orange residue was subjected to column chromatography (SiO_2 ; methanol/ MeNO_2 /2M NH_4Cl (aq), 7:1:2). Like fractions were combined, anion exchanged (NH_4PF_6), and evaporated to yield [**G1-H-G1**][PF_6]₄ as a red/orange glassy solid (0.103 g, 47%, R_f = 0.49). ^1H NMR (CD_3CN): δ = 9.33 (d, 3J = 6.9 Hz, 4H), 8.91 (d, 3J = 6.9 Hz, 4H), 8.15 (d, 3J = 6.9 Hz, 4H), 8.07 (d, 3J = 6.9 Hz, 4H), 7.46–7.35 (m, 20H), 6.77 (t, 4J = 2.2 Hz, 2H), 6.74 (d, 4J = 2.2 Hz, 4H), 6.65–6.64 (m, 4H), 6.47–6.45 (m, 4H), 5.73 (s, 4H), 5.62 (s, 4H), 5.13 (s, 8H), 4.05–4.01 ppm (m, 24H); HRMS (ESI): m/z calcd for [[**G1-H-G1**](PF_6)₃]⁺: 1829.5481; found: 1829.5514; m/z calcd for [[**G1-H-G1**](PF_6)₂]²⁺: 842.2920; found: 842.2927; m/z calcd for [[**G1-H-G1**]⁺: 348.6639; found: 348.6633.

Synthesis of rotaxane [G1-H-G1][BF₄]₄: 1,2-Bis(4,4'-bipyridinium)ethane[BF_4]₂ (0.103 g, 0.200 mmol), bromomethyl-**G1** (0.311 g, 0.814 mmol), **DB24C8** (0.182 g, 0.406 mmol), and a catalytic amount of TBAI (15 mg) were dissolved in MeCN (20 mL) and the reaction was stirred at room temperature for 7 d. The mixture was filtered and the filtrate was concentrated (3 mL) and precipitated with diethyl ether. The red/orange precipitate was filtered through Celite and washed into a clean flask with MeCN. The solvent was evaporated and the red/orange residue was subjected to column chromatography (SiO_2 ; methanol/ MeNO_2 /2M NH_4Cl (aq), 3:1:1). Like fractions were combined, anion

exchanged (NaBF₄), and evaporated to yield **G1-H-G1** (tetrafluoroborate salt) as a red/orange glassy solid (0.113 g, 33%, $R_f=0.45$). X-ray quality crystals were grown by slow diffusion of diethyl ether into a concentrated solution of [**G1-H-G1**][BF₄]₄ in MeCN. HRMS (ESI): m/z calcd for [(**G1-H-G1**)(BF₄)₃]⁺: 1655.6643; found: 1655.6611; m/z calcd for [(**G1-H-G1**)(BF₄)₂]²⁺: 784.3307; found: 784.3337.

X-ray diffraction analysis of rotaxane [G1-H-G1**][BF₄]₄:** A single crystal of [**G1-H-G1**][BF₄]₄ was frozen in paratone oil inside a cryoloop. Reflection data were integrated from frame data obtained from hemisphere scans on a Bruker APEX diffractometer with a CCD detector. Decay was monitored by 50 standard data frames measured at the beginning and end of data collection. Diffraction data and unit-cell parameters were consistent with assigned space groups. Lorentzian polarization corrections and empirical absorption corrections, based on redundant data at varying effective azimuthal angles, were applied to the data sets. The structures were solved by direct methods, completed by subsequent Fourier syntheses and refined by using full-matrix least-squares methods against $|F^2|$ data. All non-hydrogen atoms were refined anisotropically. Hydrogen atoms were treated as idealized contributions. Scattering factors and anomalous dispersion coefficients are contained in the SHELXTL 5.03 program library (G. M. Sheldrick, Madison, WI).^[22,23] Crystal data: C₉₄H₉₉N₇O₁₂B₂F₁₆Cl₂, $M_r=1915.3$, orange blocks (0.22 × 0.16 × 0.10 mm), triclinic, $P\bar{1}$, $a=10.731(2)$, $b=15.949(4)$, $c=16.299(3)$ Å, $\alpha=108.506(3)^\circ$, $\beta=101.889(2)^\circ$, $\gamma=100.471(4)^\circ$, $U=2495.0(9)$ Å³, $Z=1$, $\rho_{\text{calcd}}=1.275$ g cm⁻³, $\mu=0.155$ mm⁻¹, $\text{min trans.}=0.4847$, $\text{max trans.}=0.7457$, $2\theta_{\text{max}}=50.0^\circ$, $\text{MoK}\alpha$, $\lambda=0.71073$ Å, $T=173.0(2)$ K, 16796 total reflections ($R(\text{int})=0.0444$), $R1=0.1385$, $wR2=0.3659$ [$I>2\sigma(I)$], $R1=0.1703$, $wR2=0.3897$ (all data), $\text{GoF}(F^2)=1.165$, data/variables/restraints=8514/640/6. CCDC-744117 contains the supplementary crystallographic data for this paper. These data can be obtained free of charge from The Cambridge Crystallographic Data Centre via www.ccdc.cam.ac.uk/data_request/cif.

Synthesis of rotaxane [G2-H-G2**][PF₆]₄:** 1,2-Bis(4,4'-bipyridinium)ethane[PF₆]₂ (0.047 g, 0.0738 mmol), bromomethyl-**G2** (0.258 g, 0.319 mmol), **DB24C8** (0.076 g, 0.168 mmol), and a catalytic amount of TBAI (15 mg) were dissolved in MeNO₂ (10 mL) and CHCl₃ (10 mL). Water (10 mL) and a saturated aqueous solution of NH₄PF₆ (2 mL) were added and the two-layer reaction was stirred at room temperature for 21 d (at 7 and 14 d the aqueous layer was replaced with fresh distilled water). The organic layer was separated, dried (anhydrous MgSO₄), concentrated (2 mL), and precipitated with diethyl ether. The precipitate was filtered through Celite and washed into a clean flask with MeCN. The solvent was evaporated and the red/orange residue was subjected to column chromatography (SiO₂; methanol/MeNO₂/2M NH₄Cl (aq), 3:1:1). Like fractions were combined, anion exchanged (NH₄PF₆), and evaporated to yield [**G2-H-G2**][PF₆]₄ as a red/orange glassy solid (0.081 g, 39%, $R_f=0.43$). ¹H NMR (CD₃CN): $\delta=9.31$ (d, 4H, ³ $J=6.9$ Hz), 8.92 (d, 4H, ³ $J=6.9$ Hz), 8.13 (d, 4H, ³ $J=6.9$ Hz), 8.08 (d, 4H, ³ $J=6.9$ Hz), 7.42–7.33 (m, 40H), 6.73–6.72 (m, 6H), 6.69 (d, 8H, ⁴ $J=2.2$ Hz), 6.63–6.61 (m, 4H), 6.58 (t, 4H, ⁴ $J=2.2$ Hz), 6.47–6.45 (m, 4H), 5.73 (s, 4H), 5.60 (s, 4H), 5.06 (s, 8H), 5.05 (s, 16H), 4.05–3.99 ppm (m, 24H); HRMS (ESI): m/z calcd for [(**G2-H-G2**)(PF₆)₂]²⁺: 1266.4594; found: 1266.4589.

Synthesis of rotaxane [G3-H-G3**][PF₆]₄:** 1,2-Bis(4,4'-bipyridinium)ethane[PF₆]₂ (0.053 g, 0.0841 mmol), bromomethyl-**G3** (0.599 g, 0.362 mmol), **DB24C8** (0.076 g, 0.168 mmol), and a catalytic amount of TBAI (15 mg) were dissolved in MeNO₂ (10 mL) and CHCl₃ (10 mL). Water (10 mL) and a saturated aqueous solution of NH₄PF₆ (2 mL) were added and the two-layer reaction was stirred at room temperature for 21 d (at 3 d the aqueous layer was replaced with fresh distilled water). The organic layer was separated, dried (anhydrous MgSO₄), and concentrated. The red/orange residue was subjected to column chromatography (SiO₂; CH₂Cl₂ to EtOH in CH₂Cl₂ (5 %)). Like fractions were combined, anion exchanged (NH₄PF₆), and evaporated to yield [**G3-H-G3**][PF₆]₄ as a red/orange glassy solid (0.085 g, 22%, $R_f=0.41$). ¹H NMR (CD₃CN): $\delta=9.22$ (d, ³ $J=6.4$ Hz, 4H), 8.86 (d, ³ $J=6.4$ Hz, 4H), 8.07 (d, ³ $J=6.4$ Hz, 4H), 8.01 (d, ³ $J=6.4$ Hz, 4H), 7.38–7.27 (m, 80H), 6.71 (brs, 2H), 6.68 (brs, 4H), 6.62–6.51 (m, 40H), 6.42–6.40 (m, 4H), 5.67 (s, 4H), 5.52 (s,

4H), 5.03 (s, 8H), 5.00 (s, 32H), 4.94 (s, 16H), 3.96–3.90 ppm (m, 24H); HRMS (ESI): m/z calcd for [(**G3-H-G3**)(PF₆)₃]⁺: 2114.7943; found: 2114.7844; m/z calcd for [(**G3-H-G3**)(PF₆)₂]²⁺: 1266.4594; found: 1266.4589.

Synthesis of rotaxane [G1-G1-G1**][PF₆]₄:** 1,2-Bis(4,4'-bipyridinium)ethane[PF₆]₂ (0.043 g, 0.0682 mmol) and **G1-DB24C8** (0.106 g, 0.136 mmol) were dissolved in MeNO₂ (25 mL) and stirred for 10 min. At this point, TBAI (10 mg) and bromomethyl-**G1** (0.115 g, 0.300 mmol) were added along with water (10 mL) and a saturated aqueous solution of NH₄PF₆ (1 mL) and the two-layer reaction was then stirred at room temperature for 12 d (at 7 d the aqueous layer was replaced with fresh distilled water). The organic layer was separated, dried (anhydrous MgSO₄), concentrated (5 mL), and precipitated with diethyl ether. The red/orange precipitate was filtered through Celite and washed into a clean flask with MeCN. The solvent was evaporated and the red/orange residue was subjected to column chromatography (SiO₂; methanol/MeNO₂/2M NH₄Cl(aq), 7:1:2). Like fractions were combined, anion exchanged (NH₄PF₆), concentrated (2 mL), and precipitated from the concentrated MeNO₂ solution by slow diffusion of isopropyl ether to yield [**G1-G1-G1**][PF₆]₄ as a red/orange oil (0.090 g, 57%, $R_f=0.42$). ¹H NMR (CD₃CN): $\delta=9.32$ (d, ³ $J=6.8$ Hz, 4H), 8.82 (d, ³ $J=6.8$ Hz, 4H), 8.14 (d, ³ $J=6.8$ Hz, 4H), 8.03 (d, ³ $J=6.8$ Hz, 4H), 7.44–7.31 (m, 30H), 6.74–6.45 (m, 16H), 5.62 (s, 4H), 5.60 (s, 4H), 5.10 (s, 8H), 5.03 (s, 4H), 4.28 (s, 2H), 4.05–3.99 ppm (m, 26H); HRMS (ESI): m/z calcd for [(**G1-G1-G1**)(PF₆)₃]⁺: 2162.6893; found: 2162.6340; m/z calcd for [(**G1-G1-G1**)(PF₆)₂]²⁺: 1008.3626; found: 1008.3625; m/z calcd for [(**G1-G1-G1**)(PF₆)₃]⁺: 623.9203; found: 623.9235; m/z calcd for [(**G1-G1-G1**)]⁴⁺: 431.6992; found: 431.7012.

Synthesis of rotaxane [G2-G1-G2**][PF₆]₄:** 1,2-Bis(4,4'-bipyridinium)ethane[PF₆]₂ (0.044 g, 0.0698 mmol) and **G1-DB24C8** (0.107 g, 0.137 mmol) were dissolved in MeNO₂ (20 mL) and CHCl₃ (5 mL) and stirred for 10 min. At this point, TBAI (10 mg) and bromomethyl-**G2** (0.230 g, 0.285 mmol) were added along with water (10 mL) and a saturated aqueous solution of NH₄PF₆ (1 mL) and the two-layer reaction was stirred at room temperature for 14 d (at 7 d the aqueous layer was replaced with fresh distilled water). The organic layer was separated, dried (anhydrous MgSO₄), concentrated (5 mL), and precipitated with diethyl ether. The red/orange precipitate was filtered through Celite and washed into a clean flask with MeCN. The solvent was evaporated and the red/orange residue was heated in toluene three times, the toluene was decanted, and the solid was allowed to dry. The red/orange solid was subjected to column chromatography (SiO₂; CH₂Cl₂/EtOH, 95:5). Like fractions were combined, anion exchanged (NH₄PF₆), concentrated (2 mL), and precipitated from the concentrated solution in MeNO₂ by slow diffusion of isopropyl ether to yield [**G2-G1-G2**][PF₆]₄ as a red/orange solid (0.049 g, 22%, $R_f=0.49$). ¹H NMR (CD₃CN): $\delta=9.29$ (d, ³ $J=6.7$ Hz, 4H), 8.83 (d, ³ $J=6.7$ Hz, 4H), 8.12 (d, ³ $J=6.7$ Hz, 4H), 8.03 (d, ³ $J=6.7$ Hz, 4H), 7.40–7.31 (m, 50H), 6.71–6.53 (m, 28H), 5.63 (s, 4H), 5.58 (s, 4H), 5.03 (s, 16H), 5.02 (s, 8H), 4.96 (s, 4H), 4.22 (s, 2H), 4.04–3.95 ppm (m, 26H); HRMS (ESI): m/z calcd for [(**G2-G1-G2**)₂](PF₆)²⁺: 1432.5300; found: 1432.5309; m/z calcd for [(**G2-G1-G2**)(PF₆)₃]⁺: 906.6986; found: 906.6961; m/z calcd for [(**G2-G1-G2**)]⁴⁺: 643.7829; found: 643.7830.

Synthesis of rotaxane [G3-G1-G3**][PF₆]₄:** 1,2-Bis(4,4'-dipyridinium)ethane[PF₆]₂ (0.054 g, 0.0857 mmol) and **G3-DB24C8** (0.136 g, 0.174 mmol) were dissolved in MeNO₂ (20 mL) and stirred for 10 min. TBAI (10 mg) and bromomethyl-**G1** (0.592 g, 0.357 mmol), dissolved in CH₂Cl₂ (10 mL), were added along with water (10 mL) and a saturated aqueous solution of NH₄PF₆ (1 mL) and the two-layer reaction was stirred at room temperature for 21 d (at 3 d the aqueous layer was replaced with fresh distilled water). The organic layer was separated, dried (anhydrous MgSO₄), concentrated (2 mL), and precipitated with diethyl ether. The red/orange precipitate was filtered through Celite and washed into a clean flask with MeCN. The solvent was evaporated and the residue was subjected to column chromatography (SiO₂; CH₂Cl₂/EtOH, 95:5). Like fractions were combined, anion exchanged (NH₄PF₆), concentrated (2 mL), and precipitated from the concentrated solution in MeNO₂ by slow diffusion of isopropyl ether to yield [**G3-G1-G3**][PF₆]₄ as

a red/orange oil (0.103 g, 25%, $R_f=0.51$). $^1\text{H NMR}$ (CD_3CN): $\delta=9.23$ (d, $^3J=6.6$ Hz, 4H), 8.78 (d, $^3J=6.6$ Hz, 4H), 8.07 (d, $^3J=6.6$ Hz, 4H), 7.98 (d, $^3J=6.6$ Hz, 4H), 7.37–7.25 (m, 90H), 6.70–6.48 (m, 52H), 5.62–5.55 (m, 4H), 5.51 (s, 4H), 4.99–4.88 (m, 60H), 4.17 (s, 2H), 3.98–3.85 ppm (m, 26H); HRMS (ESI): m/z calcd for $[(\text{G3-G1-G3})(2\text{PF}_6)]^{2+}$: 2280.8649; found: 2280.8748.

Synthesis of [2]rotaxane [G1-H][PF₆]₅ and [3]rotaxane [G1-H/H][PF₆]₅: Compound **3**[PF₆]₄ (0.099 g, 0.116 mmol), **DB24C8** (0.107 g, 0.239 mmol), bromomethyl-**G1** (0.108 g, 0.282 mmol), and a catalytic amount of TBAI (10 mg) were dissolved in MeNO₂ (10 mL). Water (10 mL) and a saturated aqueous solution of NH₄PF₆ (1 mL) were added and the two-layer reaction was stirred at room temperature for 14 d (at 7 d, the aqueous layer was replaced with fresh distilled water). The organic layer was separated, dried (anhydrous MgSO₄), concentrated, and precipitated from solution by the addition of diethyl ether (40 mL). The red/orange precipitate was collected through Celite and subjected to column chromatography (SiO₂; methanol/MeNO₂/2 M NH₄Cl(aq), 7:1:2). Like fractions were collected and anion exchanged (NH₄PF₆) to yield **[G1-H][PF₆]₅** and **[G1-H/H][PF₆]₅** as red/orange glassy solids in 75% overall yield. **[G1-H][PF₆]₅** (0.049 g, 26%, $R_f=0.48$). $^1\text{H NMR}$ (CD_3CN): $\delta=9.23$ (brs, 4H), 8.99 (brs, 2H), 8.92 (d, $^3J=6.6$ Hz, 2H), 8.71 (brs, 2H), 8.22 (brs, 2H), 8.16–8.13 (m, 6H), 8.03 (brs, 2H), 7.44–7.33 (m, 10H), 6.76 (t, $^4J=2.2$ Hz, 1H), 6.72 (d, $^4J=2.2$ Hz, 2H), 6.68–6.65 (m, 4H), 6.55 (brs, 4H), 5.73 (s, 2H), 5.52 (brs, 4H), 5.28 (brs, 2H), 5.19 (brs, 2H), 5.12 (s, 4H), 4.07–3.99 (m, 24H), 1.38 ppm (brs, 9H); HRMS (ESI): m/z calcd for $[(\text{G1-H})(3\text{PF}_6)]^{2+}$: 844.7728; found: 844.7759. **[G1-H/H][PF₆]₅** (0.075 g, 49%, $R_f=0.22$); $^1\text{H NMR}$ (CD_3CN): $\delta=9.33$ –9.29 (m, 6H), 8.95 (d, $^3J=6.8$ Hz, 2H), 8.95 (d, $^3J=6.8$ Hz, 2H), 8.90 (d, $^3J=6.8$ Hz, 2H), 8.08 (d, $^3J=6.8$ Hz, 2H), 8.02 (d, $^3J=6.8$ Hz, 2H), 7.86 (d, $^3J=6.7$ Hz, 2H), 7.83 (d, $^3J=6.7$ Hz, 2H), 7.76 (d, $^3J=6.8$ Hz, 2H), 7.46–7.39 (m, 10H), 6.75–6.74 (m, 11H), 6.70–6.68 (m, 4H), 6.56–6.53 (m, 4H), 5.73 (s, 2H), 5.64–5.61 (m, 6H), 5.47–5.44 (m, 2H), 5.13 (s, 4H), 4.10–3.98 (m, 48H), 1.19 ppm (s, 9H); HRMS (ESI): m/z calcd for $[(\text{G1-H/H})(4\text{PF}_6)]^{2+}$: 2282.7196; found: 2282.7285; m/z calcd for $[(\text{G1-H/H})(3\text{PF}_6)]^{2+}$: 1068.8777; found: 1068.8715; m/z calcd for $[(\text{G1-H/H})(2\text{PF}_6)]^{2+}$: 664.2637; found: 664.2667; m/z calcd for $[(\text{G1-H/H})(\text{PF}_6)]^{4+}$: 461.9568; found: 461.9517; m/z calcd for $[(\text{G1-H/H})]^{5+}$: 340.5726; found: 340.5720.

Synthesis of [2]rotaxane [G1-G0][PF₆]₅ and [3]rotaxane [G1-G0/G0][PF₆]₅: The procedure for **[G1-H][PF₆]₅** was used with **G0-DB24C8** employed instead of **DB24C8**. **[G1-G0][PF₆]₅** and **[G1-G0/G0][PF₆]₅** were isolated as red/orange glassy products in 9% overall yield. **[G1-G0][PF₆]₅** (0.0107 g, 5%, $R_f=0.42$); $^1\text{H NMR}$ (CD_3CN): $\delta=9.24$ (brs, 4H), 8.93 (brs, 2H), 8.82 (brs, 2H), 8.66 (brs, 2H), 8.18–8.04 (brm, 10H), 7.43–7.30 (m, 15H), 6.75–6.60 (m, 8H), 6.53 (brs, 2H), 5.64 (s, 2H), 5.51 (brs, 4H), 5.18–5.11 (brs, 4H), 5.10 (s, 4H), 4.40 (s, 2H), 4.14–3.96 (m, 26H), 1.37 ppm (brs, 9H); HRMS (ESI): m/z calcd for $[(\text{G1-G0})(3\text{PF}_6)]^{2+}$: 904.8016; found: 904.8058; m/z calcd for $[(\text{G1-G0})(2\text{PF}_6)]^{2+}$: 554.8797; found: 554.8765; m/z calcd for $[(\text{G1-G0})(\text{PF}_6)]^{4+}$: 379.9187; found: 379.9184; m/z calcd for $[(\text{G1-G0})]^{5+}$: 274.9421; found: 274.9547. **[G1-G0/G0][PF₆]₅** (0.0071 g, 4%, $R_f=0.53$); $^1\text{H NMR}$ (CD_3CN): $\delta=9.33$ –9.28 (m, 6H), 8.91 (d, $^3J=6.8$ Hz, 2H), 8.76 (d, $^3J=6.5$ Hz, 2H), 8.00 (d, $^3J=5.7$ Hz, 2H), 7.96–7.91 (m, 6H), 7.72 (d, $^3J=6.8$ Hz, 2H), 7.44–7.30 (m, 20H), 6.77–6.51 (m, 17H), 5.63–5.60 (m, 8H), 5.46–5.42 (m, 2H), 5.11 (s, 4H), 4.50 (d, $J=2.7$ Hz, 2H), 4.37 (dd, $J=2.7, 4.2$ Hz, 2H), 4.34 (s, 2H), 4.13–3.93 (m, 50H), 1.14 ppm (brs, 9H); HRMS (ESI): m/z calcd for $[(\text{G1-G0/G0})(3\text{PF}_6)]^{2+}$: 1188.9352; found: 1188.9347; m/z calcd for $[(\text{G1-G0/G0})(2\text{PF}_6)]^{2+}$: 744.3021; found: 744.3076; m/z calcd for $[(\text{G1-G0/G0})(\text{PF}_6)]^{4+}$: 521.9855; found: 521.9852; m/z calcd for $[(\text{G1-G0/G0})]^{5+}$: 388.5956; found: 388.5957.

Synthesis of [2]rotaxane [G1-G1][PF₆]₅ and [3]rotaxane [G1-G1/G1][PF₆]₅: The procedure for **[G1-H][PF₆]₅** was used with **G1-DB24C8** employed instead of **DB24C8**. **[G1-G1][PF₆]₅** and **[G1-G1/G1][PF₆]₅** were isolated as red/orange glassy products in 18% overall yield. **[G1-G1][PF₆]₅** (0.0203 g, 10%, $R_f=0.42$); $^1\text{H NMR}$ (CD_3CN): $\delta=9.24$ (brs, 4H), 8.98 (brs, 2H), 8.83 (d, $^3J=5.4$ Hz, 2H), 8.69 (brs, 2H), 8.22–8.03 (brm, 10H), 7.42–7.32 (m, 20H), 6.74–6.53 (m, 13H), 5.62 (s, 2H), 5.53 (brs, 4H), 5.20 (brm, 4H), 5.09 (s, 4H), 5.04 (s, 4H), 4.34 (s, 2H), 4.13–3.92 (m, 26H), 1.36 ppm (brs, 9H); HRMS (ESI): m/z calcd for $[(\text{G1-G1})(3\text{PF}_6)]^{2+}$: 1010.8435; found: 1010.8480; m/z calcd for $[(\text{G1-G1})(2\text{PF}_6)]^{2+}$: 625.5742; found: 625.5768; m/z calcd for $[(\text{G1-G1})(\text{PF}_6)]^{4+}$: 432.9396; found: 432.9405; m/z calcd for $[(\text{G1-G1})]^{5+}$: 317.3589; found: 317.3601. **[G1-G1/G1][PF₆]₅** (0.0219 g, 8%, $R_f=0.57$); $^1\text{H NMR}$ (CD_3CN): $\delta=9.32$ –9.29 (m, 6H), 8.94 (d, $^3J=6.7$ Hz, 2H), 8.78 (d, $^3J=6.6$ Hz, 2H), 8.03 (d, $^3J=6.7$ Hz, 2H), 8.01–7.96 (m, 4H), 7.94 (d, $^3J=6.6$ Hz, 2H), 7.71 (d, $^3J=6.7$ Hz, 2H), 7.43–7.32 (m, 30H), 6.74–6.46 (m, 23H), 5.60–5.57 (m, 8H), 5.45–5.43 (m, 2H), 5.08 (s, 4H), 5.02 (s, 4H), 5.01 (s, 4H), 4.42 (d, $J=2.0$ Hz, 2H), 4.30–4.28 (m, 4H), 4.07–3.94 (m, 50H), 1.13 ppm (s, 9H); HRMS (ESI): m/z calcd for $[(\text{G1-G1/G1})(3\text{PF}_6)]^{2+}$: 1401.0189; found: 1401.0213; m/z calcd for $[(\text{G1-G1/G1})(2\text{PF}_6)]^{2+}$: 885.6912; found: 885.6932; m/z calcd for $[(\text{G1-G1/G1})(\text{PF}_6)]^{4+}$: 628.0274; found: 628.0281; m/z calcd for $[(\text{G1-G1/G1})]^{5+}$: 473.4291; found: 473.4298.

Synthesis of [2]rotaxane [G1-G2][PF₆]₅ and [3]rotaxane [G1-G2/G2][PF₆]₅: Compound **3**[PF₆]₄ (0.051 g, 0.059 mmol), **G2-DB24C8** (0.137 g, 0.114 mmol) were dissolved in MeNO₂ (15 mL) and stirred for 5 min. Bromomethyl-**G1** (0.049 g, 0.128 mmol), water (10 mL), and NH₄PF₆(aq) (1 mL) were added and the two-layer reaction stirred at room temperature for 21 d. The organic layer was separated, washed with water (3 × 50 mL), dried (anhydrous MgSO₄), and concentrated. The orange residue was sonicated in toluene (3 × 20 mL) and the toluene was decanted and the residue was air dried. The residue was washed with MeCN (2 mL), the remaining yellow solid was filtered and the filtrate was concentrated to give a red/orange residue, which was subjected to column chromatography (SiO₂; 0.025 M NH₄PF₆ in MeCN/CH₂Cl₂, 3:2). Like fractions (as determined by NMR) were collected, anion exchanged (NH₄PF₆) and precipitated from MeCN by slow diffusion of isopropyl ether to yield **[G1-G2][PF₆]₅** and **[G1-G2/G2][PF₆]₅** as red/orange glassy products in 15% overall yield. **[G1-G2][PF₆]₅** (0.0161 g, 10% $R_f=0.41$). $^1\text{H NMR}$: (CD_3CN) $\delta=9.22$ (brs, 4H), 8.93 (brs, 2H), 8.77 (brs, 2H), 8.64 (brs, 2H), 8.23–8.03 (brm, 10H), 7.40–7.29 (m, 30H), 6.75–6.54 (m, 19H), 5.57–5.52 (brm, 6H), 5.16–5.12 (brm, 4H), 5.05 (s, 4H), 5.02 (s, 8H), 4.98 (s, 4H), 4.33 (s, 2H), 4.11–3.88 (m, 26H), 1.36 ppm (brs, 9H). HRMS (ESI): m/z calcd for $[(\text{G1-G2})(3\text{PF}_6)]^{2+}$: 1222.9272; found: 1222.9292; m/z calcd for $[(\text{G1-G2})(2\text{PF}_6)]^{2+}$: 766.9634; found: 766.9653; m/z calcd for $[(\text{G1-G2})(\text{PF}_6)]^{4+}$: 538.9815; found: 538.9793; m/z calcd for $[(\text{G1-G2})]^{5+}$: 402.1924; found: 402.1927. **[G1-G2/G2][PF₆]₅** (0.0115 g, 5% $R_f=0.58$); $^1\text{H NMR}$ (CD_3CN): $\delta=9.32$ –9.29 (m, 6H), 8.94 (d, $^3J=6.7$ Hz, 2H), 8.78 (d, $^3J=6.6$ Hz, 2H), 8.03 (d, $^3J=6.7$ Hz, 2H), 8.01–7.96 (m, 4H), 7.94 (d, $^3J=6.6$ Hz, 2H), 7.71 (d, $^3J=6.7$ Hz, 2H), 7.43–7.32 (m, 30H), 6.74–6.46 (m, 23H), 5.60–5.57 (m, 8H), 5.45–5.43 (m, 2H), 5.08 (s, 4H), 5.02 (s, 4H), 5.01 (s, 4H), 4.42 (d, $J=2.0$ Hz, 2H), 4.30–4.28 (m, 4H), 4.07–3.94 (m, 50H), 1.13 ppm (s, 9H); HRMS (ESI): m/z calcd for $[(\text{G1-G2/G2})(3\text{PF}_6)]^{2+}$: 1825.1864; found: 1825.1913; m/z calcd for $[(\text{G1-G2/G2})(2\text{PF}_6)]^{2+}$: 1168.4695; found: 1168.4714; m/z calcd for $[(\text{G1-G2/G2})(\text{PF}_6)]^{4+}$: 840.1111; found: 840.1149; m/z calcd for $[(\text{G1-G2/G2})]^{5+}$: 643.0961; found: 643.0946.

Synthesis of [2]rotaxane [G2-H][PF₆]₅ and [3]rotaxane [G2-H/H][PF₆]₅: Compound **3**[PF₆]₄ (0.0673 g, 0.0792 mmol), **DB24C8** (0.107 g, 0.239 mmol), bromomethyl-**G2** (0.159 g, 0.179 mmol), and a catalytic amount of TBAI (10 mg) were dissolved in MeNO₂ (20 mL) and CHCl₃ (3 mL). Water (10 mL) and a saturated aqueous solution of NH₄PF₆ (2 mL) were added and the two-layer reaction stirred at room temperature for 14 d (at 7 d the aqueous layer was replaced with fresh distilled water). The organic layer was separated, dried (anhydrous MgSO₄), concentrated (3 mL), and precipitated from solution with the addition of diethyl ether (50 mL). The red/orange precipitate was collected through Celite and subjected to column chromatography (SiO₂; methanol/MeNO₂/2 M NH₄Cl (aq), 7:1:2). Like fractions were collected and anion exchanged (NH₄PF₆) to yield **[G2-H][PF₆]₅** and **[G2-H/H][PF₆]₅** as red/orange glassy solids in 18% overall yield. **[G2-H][PF₆]₅** (0.0226 g, 10%, $R_f=0.51$); $^1\text{H NMR}$ (CD_3CN): $\delta=9.22$ (brs, 4H), 8.98 (brs, 2H), 8.91 (d, $^3J=6.7$ Hz, 2H), 8.70 (brs, 2H), 8.18–8.04 (brm, 10H), 7.41–7.31 (m, 20H), 6.70 (s, 3H), 6.67 (d, $^3J=2.2$ Hz, 4H), 6.66–6.64 (m, 4H), 6.57 (t, $^3J=2.2$ Hz, 2H), 6.53 (brs, 4H), 5.72 (s, 2H), 5.51 (brs, 4H), 5.19 (brs, 4H), 5.04 (s, 12H), 4.06–3.95 (m, 24H), 1.37 ppm (s, 9H); HRMS (ESI): m/z calcd for $[(\text{G2-H})(3\text{PF}_6)]^{2+}$: 1056.8566; found: 1056.8572; m/z calcd for $[(\text{G2-H})(2\text{PF}_6)]^{2+}$: 656.2497; found: 656.2512; m/z calcd for $[(\text{G2-H})(\text{PF}_6)]^{4+}$: 455.9462; found: 455.9470; m/z calcd for $[(\text{G2-H})]^{5+}$: 335.7641;

found: 335.7646. [**G2-H/H**][PF₆]₅ (0.0151 g, 8%, $R_f=0.24$); ¹H NMR (CD₃CN): δ=9.32–9.27 (m, 6H), 8.92 (d, ³J=6.8 Hz, 2H), 8.89 (d, ³J=6.7 Hz, 2H), 8.03 (d, ³J=6.7 Hz, 2H), 7.99 (d, ³J=6.7 Hz, 2H), 7.85 (d, ³J=6.7 Hz, 2H), 7.82 (d, ³J=6.7 Hz, 2H), 7.75 (d, ³J=6.8 Hz, 2H), 7.42–7.32 (m, 20H), 6.73 (s, 8H), 6.71 (s, 3H), 6.68 (d, $J=2.3$ Hz, 4H), 6.67–6.65 (m, 4H), 6.57 (t, $J=2.3$ Hz, 2H), 6.54–6.51 (m, 4H), 5.72 (s, 2H), 5.63–5.59 (m, 6H), 5.46–5.42 (m, 2H), 5.05 (s, 4H), 5.04 (s, 8H), 4.08–3.97 (m, 48H), 1.17 ppm (s, 9H); HRMS (ESI): m/z calcd for [(**G2-H/H**)(PF₆)₂]³⁺: 1280.9614; found: 1280.9652; m/z calcd for [(**G2-H/H**)(PF₆)₂]³⁺: 805.6529; found: 805.6569; m/z calcd for [(**G2-H/H**)(PF₆)₂]⁴⁺: 567.9986; found: 567.9973; m/z calcd for [(**G2-H/H**)]³⁺: 425.4061; found: 425.4064.

Synthesis of [2]rotaxane [G2-G0][PF₆]₅ and [3]rotaxane [G2-G0/G0]-[PF₆]₅: The same procedure as that used for [**G2-H**][PF₆]₅ and [**G2-H/H**]-[PF₆]₅ was used with **G0-DB24C8** instead of **DB24C8**. [**G2-G0**][PF₆]₅ and [**G2-G0/G0**][PF₆]₅ were isolated as red/orange glassy solids in 12% overall yield. [**G2-G0**][PF₆]₅ (0.0088 g, 6%, $R_f=0.50$); ¹H NMR (CD₃CN): δ=9.20 (brs, 4H), 8.91 (brs, 2H), 8.80 (m, 2H), 8.62 (brs, 2H), 8.23–7.98 (m, 10H), 7.37–7.29 (m, 25H), 6.70–6.47 (m, 16H), 5.59 (s, 2H), 5.52 (brs, 4H), 5.22–5.15 (m, 4H), 5.02–4.99 (m, 12H), 4.28 (s, 2H), 4.10–3.85 (m, 26H), 1.38 ppm (brs, 9H); HRMS (ESI): m/z calcd for [(**G2-G0**)(PF₆)₂]²⁺: 1116.8848; found: 1116.8890; m/z calcd for [(**G2-G0**)(PF₆)₂]³⁺: 696.2683; found: 696.2710; m/z calcd for [(**G2-G0**)(PF₆)₂]⁴⁺: 485.9600; found: 485.9609; m/z calcd for [(**G2-G0**)]³⁺: 359.7751; found: 359.7746. [**G2-G0/G0**][PF₆]₅ (0.0107 g, 6%, $R_f=0.66$); ¹H NMR (CD₃CN): δ=9.32 (d, ³J=6.6 Hz, 2H), 9.28 (d, ³J=6.6 Hz, 2H), 9.27 (d, ³J=6.6 Hz, 2H), 8.93 (d, ³J=6.6 Hz, 2H), 8.76 (d, ³J=6.6 Hz, 2H), 7.94–7.90 (m, 4H), 7.89–7.85 (m, 4H), 7.72 (d, ³J=6.6 Hz, 2H), 7.40–7.30 (m, 30H), 6.72–6.43 (m, 23H), 5.61–5.56 (m, 8H), 5.44–5.40 (m, 2H), 5.00 (s, 8H), 4.96 (s, 4H), 4.43 (d, $J=2.2$ Hz, 2H), 4.29 (d, $J=5.5$ Hz, 2H), 4.25 (s, 2H), 4.04–3.94 (m, 50H), 1.13 ppm (s, 9H); HRMS (ESI): m/z calcd for [(**G2-G0/G0**)(PF₆)₂]²⁺: 1401.0184; found: 1401.0177; m/z calcd for [(**G2-G0/G0**)(PF₆)₂]³⁺: 995.6907; found: 995.6914; m/z calcd for [(**G2-G0/G0**)(PF₆)₂]⁴⁺: 628.0268; found: 628.0270.

Synthesis of [2]rotaxane [G2-G1][PF₆]₅ and [3]rotaxane [G2-G1/G1]-[PF₆]₅: Compound **3**[PF₆]₄ (0.061 g, 0.072 mmol) and **G1-DB24C8** (0.121 g, 0.155 mmol) were dissolved in MeNO₂ (20 mL) and stirred for 5 min. Bromomethyl-**G2** (0.127 g, 0.157 mmol), a catalytic amount of TBAI (10 mg), water (15 mL), CH₂Cl₂ (2 mL), and NH₄PF₆ (aq) (1 mL) were added and the two-layer reaction stirred at room temperature for 21 d. The organic layer was separated, washed with water (2×50 mL), dried (anhydrous MgSO₄), concentrated (2 mL), and precipitated from solution with diethyl ether (3×40 mL). The red/orange precipitate was collected through Celite and subjected to column chromatography (SiO₂; 0.025 M NH₄PF₆ in MeCN/CH₂Cl₂, 7:3 to 3:2). Like fractions (as determined by NMR) were collected, anion exchanged (NH₄PF₆), and precipitated from MeNO₂ by slow diffusion of isopropyl ether to yield [**G2-G1**]-[PF₆]₅ and [**G2-G1/G1**][PF₆]₅ as red/orange glassy solids in 10% overall yield. [**G2-G1**][PF₆]₅ (0.0075 g, 4%, $R_f=0.44$); ¹H NMR (CD₃CN): δ=9.21 (brs, 4H), 8.92 (brs, 2H), 8.80 (m, 2H), 8.64 (brs, 2H), 8.22–7.99 (m, 10H), 7.38–7.30 (m, 30H), 6.69–6.47 (m, 19H), 5.59 (s, 2H), 5.52 (brs, 4H), 5.21–5.13 (m, 4H), 5.03–4.99 (m, 16H), 4.28 (s, 2H), 4.11–3.87 (m, 26H), 1.37 ppm (brs, 9H); HRMS (ESI): m/z calcd for [(**G2-G1**)(PF₆)₂]³⁺: 1222.9272; found: 1222.9296; m/z calcd for [(**G2-G1**)(PF₆)₂]³⁺: 766.9634; found: 766.9647; m/z calcd for [(**G2-G1**)(PF₆)₂]⁴⁺: 538.9815; found: 538.9841; m/z calcd for [(**G2-G1**)]³⁺: 402.1924; found: 402.1940. [**G2-G1/G1**][PF₆]₅ (0.0138 g, 6%, $R_f=0.59$); ¹H NMR (CD₃CN): δ=9.31 (d, ³J=6.5 Hz, 2H), 9.28 (d, ³J=6.7 Hz, 2H), 9.26 (d, ³J=6.7 Hz, 2H), 8.91 (d, ³J=6.7 Hz, 2H), 8.75 (d, ³J=6.4 Hz, 2H), 7.94–7.92 (m, 4H), 7.90–7.86 (m, 4H), 7.72 (d, ³J=6.7 Hz, 2H), 7.40–7.29 (m, 40H), 6.74–6.44 (m, 29H), 5.61–5.56 (m, 8H), 5.44–5.40 (m, 2H), 5.02 (s, 4H), 5.01 (s, 4H), 5.00 (s, 8H), 4.96 (s, 4H), 4.43 (d, $J=2.0$ Hz, 2H), 4.29 (d, $J=5.9$ Hz, 2H), 4.25 (s, 2H), 4.06–3.93 (m, 50H), 1.14 ppm (s, 9H); HRMS (ESI): m/z calcd for [(**G2-G1/G1**)(PF₆)₂]²⁺: 1613.1027; found: 1613.0958; m/z calcd for [(**G2-G1/G1**)(PF₆)₂]³⁺: 1027.0804; found: 1027.0823; m/z calcd for [(**G2-G1/G1**)(PF₆)₂]⁴⁺: 734.0692; found: 734.0714.

Synthesis of [2]rotaxane [G2-G2][PF₆]₅ and [3]rotaxane [G2-G2/G2]-[PF₆]₅: Compound **3**[PF₆]₄ (0.049 g, 0.058 mmol) and **G2-DB24C8** (0.137 g, 0.114 mmol) were dissolved in MeNO₂ (20 mL) and stirred for

5 min. Bromomethyl-**G2** (0.094 g, 0.116 mmol), dissolved in CH₂Cl₂ (3 mL), a catalytic amount of TBAI (5 mg), water (10 mL), and a saturated aqueous solution of NH₄PF₆ (1 mL) were added and the two-layer reaction stirred at room temperature for 21 d. The organic layer was separated, washed with water (3×50 mL), dried (anhydrous MgSO₄), and concentrated. The orange residue was dissolved in a minimum amount of MeCN/toluene (5 mL) and diethyl ether was added to precipitate an orange solid, which was collected through Celite and stirred in methanol (20 mL). The methanol was decanted and the residue was air dried before being subjected to column chromatography (SiO₂; 0.025 M NH₄PF₆ in MeCN/CH₂Cl₂, 3:2). Like fractions (as determined by NMR spectroscopy) were collected, anion exchanged (NH₄PF₆), and precipitated from MeCN by slow diffusion of isopropyl ether to yield [**G2-G2**][PF₆]₅ and [**G2-G2/G2**][PF₆]₅ as red/orange glassy products in 17% overall yield. [**G2-G2**][PF₆]₅ (0.0201 g, 11% $R_f=0.39$); ¹H NMR (CD₃CN): δ=9.30–9.21 (m, 4H), 8.91 (brs, 2H), 8.72 (brs, 2H), 8.62 (brs, 2H), 8.25–8.22 (m, 4H), 8.07–7.89 (m, 6H), 7.40–7.29 (m, 40H), 6.66–6.51 (m, 25H), 5.55–5.52 (m, 6H), 5.19–5.11 (m, 4H), 5.03–4.90 (m, 24H), 4.24 (s, 2H), 4.07–3.94 (m, 26H), 1.39 ppm (brs, 9H); HRMS (ESI): m/z calcd for [(**G2-G2**)(PF₆)₂]³⁺: 908.3526; found: 908.3544; m/z calcd for [(**G2-G2**)(PF₆)₂]⁴⁺: 645.0234; found: 645.0221; m/z calcd for [(**G2-G2**)]³⁺: 487.0259; found: 487.0271. [**G2-G2/G2**][PF₆]₅ (0.0147 g, 6% $R_f=0.57$); ¹H NMR (CD₃CN): δ=9.29 (d, ³J=6.5 Hz, 2H), 9.25 (d, ³J=6.3 Hz, 2H), 9.22 (d, ³J=6.5 Hz, 2H), 8.90 (d, ³J=6.7 Hz, 2H), 8.70 (d, ³J=6.4 Hz, 2H), 7.91–7.87 (m, 6H), 7.81 (d, ³J=6.4 Hz, 2H), 7.72 (d, ³J=6.7 Hz, 2H), 7.38–7.28 (m, 60H), 6.71–6.48 (m, 41H), 5.57–5.52 (m, 8H), 5.40–5.38 (m, 2H), 5.01–4.86 (m, 36H), 4.41 (brs, 2H), 4.27 (d, $J=5.4$ Hz, 2H), 4.21 (d, $J=2.8$ Hz, 2H), 4.02–3.90 (m, 50H), 1.15 ppm (s, 9H); HRMS (ESI): m/z calcd for [(**G2-G2/G2**)(PF₆)₂]³⁺: 1309.8587; found: 1309.8571; m/z calcd for [(**G2-G2/G2**)(PF₆)₂]⁴⁺: 946.1529; found: 946.1552; [(**G2-G2/G2**)]³⁺: 727.9295; found: 727.9299.

Acknowledgements

S.J.L. is grateful to the NSERC of Canada for awarding of a Discovery Grant in support of this research.

- [1] a) J. F. Stoddart, *Chem. Soc. Rev.* **2009**, *38*, 1802; b) E. R. Kay, D. A. Leigh, *Pure Appl. Chem.* **2008**, *80*, 17; c) V. Balzani, A. Credi, M. Venturi, M. *Molecular Devices and Machines: A Journey into the Nano World*, Wiley-VCH, Weinheim, **2008**; d) V. Serreli, C.-F. Lee, E. R. Kay, D. A. Leigh, *Nature* **2007**, *445*, 523; e) S. Saha, J. F. Stoddart, *Chem. Soc. Rev.* **2007**, *36*, 77.
- [2] For a recent example and detailed explanation of this phenomenon, see: J. M. Spruell, W. F. Paxton, J.-C. Olsen, D. Benítez, E. Tkatchouk, C. L. Stern, A. Trabolsi, D. C. Friedman, W. A. Goddard III, J. F. Stoddart, *J. Am. Chem. Soc.* **2009**, *131*, 11571.
- [3] For recent examples, see: a) D. C. Jagesar, S. M. Fazio, J. Taybi, E. Eiser, F. G. Gatti, D. A. Leigh, A. M. Brouwer, *Adv. Funct. Mater.* **2009**, *19*, 3440; b) I. Aprahamian, T. Yasuda, T. Ikeda, S. Saha, W. R. Dichtel, K. Isoda, T. Kato, J. F. Stoddart, *Angew. Chem.* **2007**, *119*, 4759; *Angew. Chem. Int. Ed.* **2007**, *46*, 4675; c) E. D. Baranoff, J. Voignier, T. Yasuda, V. Heitz, J.-P. Sauvage, T. Kato, *Angew. Chem.* **2007**, *119*, 4764; *Angew. Chem. Int. Ed.* **2007**, *46*, 4680; d) A. B. Braunschweig, B. H. Northrop, J. F. Stoddart, *J. Mater. Chem.* **2006**, *16*, 32.
- [4] E. R. Kay, D. A. Leigh, F. Zerbetto, *Angew. Chem.* **2007**, *119*, 72; *Angew. Chem. Int. Ed.* **2007**, *46*, 72.
- [5] a) S. J. Loeb, J. A. Wisner, *Angew. Chem.* **1998**, *110*, 3010; *Angew. Chem. Int. Ed.* **1998**, *37*, 2838; b) D. J. Hoffart, S. J. Loeb, A. de La Torre, J. Tiburcio, *Angew. Chem.* **2008**, *120*, 103; *Angew. Chem. Int. Ed.* **2008**, *47*, 97.
- [6] For recent examples of the use of Fréchet-type dendrons, see: a) D. Alivertis, G. Paraskevopoulos, V. Theodorou, K. Skobridis, *Tetrahedron Lett.* **2009**, *50*, 6019; b) D. Xu, W. Wang, D. Gesua, A. E. Kaifer, *Org. Lett.* **2008**, *10*, 4517; c) P. Bhattacharya, A. E. Kaifer, J.

- Org. Chem.* **2008**, *73*, 5693; d) H.-B. Yang, B. H. Northrop, Y.-R. Zheng, K. Ghosh, P. J. Stang, *J. Org. Chem.* **2009**, *74*, 7067.
- [7] For examples of rotaxanes and catenanes containing dendritic appendages, see: a) D. B. Amabilino, P. R. Ashton, V. Balzani, C. L. Brown, A. Credi, J. M. J. Fréchet, J. W. Leon, M. Raymo, N. Spencer, J. F. Stoddart, M. Venturi, *J. Am. Chem. Soc.* **1996**, *118*, 12012; b) C. Reuter, G. Pawlitzki, U. Wörsdörfer, M. Plevoets, A. Mohry, T. Kubota, Y. Okamoto, F. Vögtle, *Eur. J. Org. Chem.* **2000**, 3059; c) A. M. Elizarov, S.-H. Chiu, P. T. Glink, J. F. Stoddart, *Org. Lett.* **2002**, *4*, 679; d) A. M. Elizarov, T. Chjang, S.-H. Chiu, J. F. Stoddart, *Org. Lett.* **2002**, *4*, 3565.
- [8] S. J. Loeb, J. A. Wisner, *Chem. Commun.* **1998**, 2757.
- [9] S. J. Loeb, J. Tiburcio, S. J. Vella, J. A. Wisner, *Org. Biomol. Chem.* **2006**, *4*, 667.
- [10] a) S. J. Loeb, *Chem. Commun.* **2005**, 1511; b) D. J. Hoffart, S. J. Loeb, *Angew. Chem.* **2005**, *117*, 923; *Angew. Chem. Int. Ed.* **2005**, *44*, 901; c) G. J. E. Davidson, S. J. Loeb, S. J. *Angew. Chem.* **2003**, *115*, 78; *Angew. Chem. Int. Ed.* **2003**, *42*, 74. S. J. Loeb, *Chem. Soc. Rev.* **2007**, *36*, 226; d) G. J. E. Davidson, S. J. Loeb, P. Passaniti, S. Silva, A. Credi, *Chem. Eur. J.* **2006**, *12*, 3233; e) N. Georges, S. J. Loeb, J. Tiburcio, J. A. Wisner, *Org. Biomol. Chem.* **2004**, *2*, 2751.
- [11] Molecular mechanics calculations were performed using the MM3 force-field in the program CAChe; Biosciences Group, Fujitsu Computer Systems Corp., Westwood, MA. X-ray coordinates for the [2]pseudorotaxane 1^{2+} were used as the starting point for all calculations.
- [12] a) P. L. Anelli, N. Spencer, J. F. Stoddart, *J. Am. Chem. Soc.* **1991**, *113*, 5131; b) P. R. Ashton, D. Philp, N. Spencer, J. F. Stoddart, *J. Chem. Soc. Chem. Commun.* **1992**, 1124.
- [13] S. J. Loeb, J. A. Wisner, *Chem. Commun.* **2000**, 1939.
- [14] S. J. Loeb, J. A. Wisner, *Chem. Commun.* **2000**, 845.
- [15] For an example of a liquid crystalline molecular shuttle, see: a) I. Aprahamian, T. Yasuda, T. Ikeda, S. Saha, W. R. Dichtel, K. Isoda, T. Kato, J. F. Stoddart, *Angew. Chem.* **2007**, *119*, 4759; *Angew. Chem. Int. Ed.* **2007**, *46*, 4675. For examples of molecular shuttles in polymers, see: b) D. A. Leigh, M. A. F. Morales, E. M. Perez, J. K. Y. Wong, C. G. Saiz, A. M. Z. Slawin, A. J. Carmichael, D. M. Haddleton, A. M. Brouwer, W. J. Buma, G. W. H. Wurpel, S. Leon, F. Zerbetto, *Angew. Chem.* **2005**, *117*, 3122; *Angew. Chem. Int. Ed.* **2005**, *44*, 3062; c) K. Nørgaard, B. W. Laursen, S. Nygaard, K. Kjaer, H.-R. Tseng, A. H. Flood, J. F. Stoddart, T. Bjoernholm, *Angew. Chem.* **2005**, *117*, 7197; *Angew. Chem. Int. Ed.* **2005**, *44*, 7035.
- [16] For a recent review on a biologically relevant chemical system, see: a) I. Saraogi, A. D. Hamilton, *Chem. Soc. Rev.* **2009**, *38*, 1726; b) For a recent review on a biological system, see: A. Abedini, D. P. Raleigh, *Protein Eng. Des. Sel.* **2009**, *22*, 453.
- [17] gNMR, Version 5, Adept Scientific Inc. Bethesda, MD, **2003**.
- [18] C. J. Hawker, J. M. J. Fréchet, *J. Am. Chem. Soc.* **1990**, *112*, 7638.
- [19] S. J. Loeb, D. A. Tramontozzi, *Org. Biomol. Chem.* **2005**, *3*, 1393.
- [20] M. I. Attalla, N. S. McAlpine, L. A. Summers, *Z. Naturforsch. B* **1984**, *39*, 74.
- [21] D. A. Tramontozzi, Ph.D. Thesis, **2004**, University of Windsor, Windsor.
- [22] G. M. Sheldrick, *Acta Crystallogr. Sect. A* **2008**, *64*, 112.
- [23] DIAMOND 3.2—CRYSTAL IMPACT, Bonn, **2009**.

Received: November 18, 2009
Published online: March 29, 2010